Calculations of α-decay half-lives for heavy and superheavy nuclei

Yibin Qian,[1,*] Zhongzhou Ren,[1,2,3,†] and Dongdong Ni[1]
[1]*Department of Physics, Nanjing University, Nanjing 210093, China*
[2]*Kavli Institute for Theoretical Physics China, Beijing 100190, China*
[3]*Center of Theoretical Nuclear Physics, National Laboratory of Heavy-Ion Accelerator, Lanzhou 730000, China*
(Received 24 January 2011; revised manuscript received 29 March 2011; published 25 April 2011)

Systematic calculations on the α-decay half-lives of heavy and superheavy nuclei are performed within a deformed version of the cluster model, using the modified two-potential approach. The deformed Woods-Saxon potential is employed to calculate the α-decay width through a deformed barrier. For comparison the calculated α-decay half-lives in the empirical relations are also presented. The present study is initially restricted to even-even nuclei in the heavy mass region with $N > 126$. Then the study is extended to the recentlyobserved heaviest nuclei, including synthesized superheavy elements and isotopes. The α-decay half-lives obtained are found to be in good agreement with the experimental data.

DOI: 10.1103/PhysRevC.83.044317 PACS number(s): 23.60.+e, 21.10.Tg, 21.60.Gx, 27.90.+b

I. INTRODUCTION

The study of α decay dates back to the early days of nuclear physics, even to the first observation of unknown radiation by Becquerel in 1896. With the foundation and development of quantum mechanics, Gamow [1] and Condon and Gurney [2] independently described α decay as a quantum tunneling problem for the first time in 1928. These pioneering works were the first successful applications of quantum mechanics to nuclear physics. Different from the cluster model based on the Gamow picture, some other theoretical models, such as the shell model and the fissionlike model, have also been proposed in the pursuit of a microscopic description of α decay. Consequently, the absolute α-decay width has been estimated by many theoretical calculations [3–17], which employ various approaches such as the WKB method [4–7], the distorted-wave Born approximation [13], the coupled-channel approach [14,15], and phenomenological methods [16,17]. On the experimental side, as an engaging topic in contemporary nuclear physics, the observation of α-decay chains from unknown parent nuclei to known nuclei has been a reliable method used to identify different superheavy elements (SHEs) and isomeric states [18–21]. In addition, α emissions are helpful in the research of the exotic molecular states in light nuclei [22]. Moreover, α decay, as one of the most important decay modes for unstable nuclei, has long been a useful and precise tool in the investigation of nuclear structure [23–27]. For example, measurements of α decay in the closed-shell region around $Z = 82$ can provide unique shell structure information [23,24] and also give an opportunity to find a triplet of differently shaped states [27].

Based on the Gamow model, the α-decay process is usually considered as one preformed α particle tunneling through the potential barrier between the cluster and the daughter nucleus. Obviously, the α-preformation factor is indispensable for the calculations of α-decay half-lives. However, it is actually difficult to obtain the quantity due to the complexity of the nuclear many-body problem. Plenty of theoretical attempts have been made to achieve the goal. Several approaches have been developed for this purpose [25], e.g., the shell model in combination with the BCS method [28] and the hybrid model supplementing the shell-model wave function with a cluster component [3]. At present, the microscopic calculation (the hybrid model) indicates that the weight of clustering is as high as 0.3 for the typical nucleus ^{212}Po with two protons and two neutrons outside the double magic shell. Alternatively, the formation factor may also be extracted from the ratios of the experimental α-decay width to the penetration probability [5,29,30], considering that the absolute α-decay width is mainly determined by the formation factor and the barrier penetration probability within the Gamow model.

As mentioned in Refs. [31,32], the tunneling problem can be simply treated by reducing it to two separate problems: the bound-state problem and the scattering-state problem. This can be achieved consistently by the two-potential approach (TPA), which is a fully quantum method based on the perturbation theory. Moreover, the TPA not only provides good physical insight, but it is simple and accurate as well [32]. Very recently we employed the two-potential approach to evaluate the α-decay half-lives of medium mass nuclei within the cluster model, including the exotic nuclei around the $N =$ 126 shell closure [33,34]. The calculated results of medium nuclei are found to agree well with the experimental data. This has encouraged us to extend the previous work to the heavy and superheavy regions. In addition, Gurvitz *et al.* have proposed further developments for the TPA, which provide a detailed discussion on the corrections to the TPA and a modified form resembling the R-matrix theory without losing its accuracy [32]. In the present study we use the modified two-potential approach (MTPA) within the cluster model to give a description of α decay. Meanwhile, we extend the approach for the system composed of the α particle and the deformed daughter nucleus. The α-core nuclear potential is obtained in a deformed potential of the Woods-Saxon shape, which has achieved remarkable success in both nuclear structure and nuclear reactions [13]. In order to obtain the α-decay width, the numerical solution of the radial Schrödinger equation for the bound state is preformed. In addition, we employ the

*qyibin@gmail.com
†zren@nju.edu.cn

Viola-Seaborg formula to evaluate the α-decay half-lives for comparison. This famous Viola-Seaborg formula [35] has been widely used for α decay [36,37] and is also extended to cluster radioactivity [38]. Recently, other empirical relations were developed by Denisov and Khudenko [16] and Royer [17], which introduced the terms related to the angular momentum and parity of α transition, to evaluate the partial α-decay half-lives. These two analytical formulas give similarly good agreement between the evaluated results and the experimental data.

This article is organized as follows. In Sec. II the theoretical framework of the calculation of α-decay half-lives is briefly described. In Sec. III we present numerical results and detailed discussion for heavy and superheavy nuclei, including the recently observed SHEs. A brief summary is given in Sec. IV.

II. THEORETICAL FRAMEWORK

Consider a quantum well $V(r)$ with a barrier, which contains a quasistationary state at E. The coordinate space can be divided into two regions by a separation radius R. Correspondingly, one introduces two auxiliary potentials [31,32]: the inner potential

$$U(r) = \begin{cases} V(r), & r \leqslant R \\ V(R) = V_0, & r > R \end{cases} \tag{1}$$

and the outer potential

$$W(r) = \begin{cases} 0, & r \leqslant R \\ V(r) - V_0, & r > R. \end{cases} \tag{2}$$

The separation radius R is taken inside the barrier of the total interaction potential V (Fig. 1). As additional information we introduce a shifted potential $\tilde{W}(r) = W(r) + V_0$, which vanishes for $r \to \infty$, to solve the eigenproblem perturbatively in the TPA since the perturbation $W(r) \to -V_0$ at $r \to \infty$ [31,32].

To extend the α-decay width for the deformed case we assume an α particle interacts with an axially symmetric deformed daughter nucleus. The total interaction potential, including the attractive part, the repulsive Coulomb part, and the additional centrifugal part, is given by

$$V(r,\theta) = V_N(r,\theta) + V_C(r,\theta) + \frac{\hbar^2 \ell(\ell+1)}{2\mu r^2}, \tag{3}$$

where θ is the orientation angle of the emitted α particle with respect to the symmetric axis of the deformed daughter nucleus and ℓ is the angular momentum carried by the α particle. The nuclear potential is given by the Woods-Saxon type potential

$$V_N(r,\theta) = \frac{V_0}{1 + \exp\left(\frac{r - R(\theta)}{a}\right)}, \tag{4}$$

where the radius parameter $R(\theta) = R_0[1 + \beta_2 Y_{20}(\theta) + \beta_4 Y_{40}(\theta)]$ fm, $R_0 = 1.18 A_d^{1/3}$, and the diffuseness $a = 0.6$ fm. These Woods-Saxon parameter values are consistent with those of Refs. [13,39]. Here A_d, β_2, and β_4 are, respectively, the mass number, the quadrupole deformation parameter, and the hexadecapole deformation parameter of the daughter nucleus. The deformation parameters are taken from the work of Möller

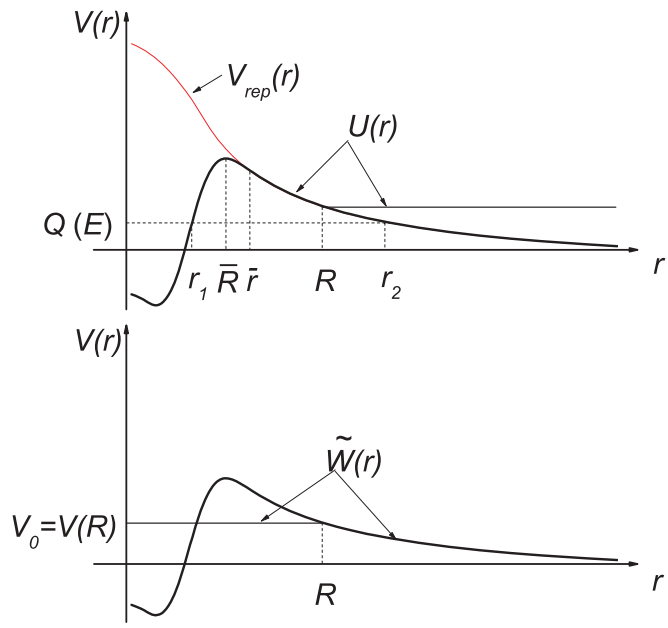

FIG. 1. (Color online) In the spherical (i.e., one-dimensional) case, for $r > \bar{r}$ the total potential $V(r)$ can be approximated by its repulsive part $V_{\rm rep}(r)$. $r_{1,2}$ denote the classical turning points $[V(r_1), V(r_2) = Q]$. Also shown are the inner potential U (top) and the introduced potential $\tilde{W}$ (bottom). It is evident that the separation radius R should be taken away from r_1, but not too close to r_2, to achieve corrections to the TPA [32].

et al. [40]. The deformed Coulomb term is taken as the form of Refs. [11,12]:

$$V_C(r,\theta) = \frac{Z_d Z_\alpha e^2}{r}\left(1 + \frac{3R_0^2}{5r^2}\beta_2 Y_{20}(\theta) + \frac{3R_0^4}{9r^4}\beta_4 Y_{40}(\theta)\right) \tag{5}$$

for $r > R(\theta)$ and

$$V_C(r,\theta) \approx \frac{Z_d Z_\alpha e^2}{2R(\theta)}\left[3 - \frac{r^2}{R(\theta)^2} + \frac{6R_0^2}{5R(\theta)^2}\beta_2 Y_{20}(\theta) \times \left(2 - \frac{r^3}{R(\theta)^3}\right) + \frac{3R_0^4}{9R(\theta)^4}\beta_4 Y_{40}(\theta)\left(7 - \frac{5r^2}{R(\theta)^2}\right)\right] \tag{6}$$

for $r \leqslant R(\theta)$.

For a certain orientation angle θ of the α particle, one can correspondingly obtain a result for the decay width by following the MTPA procedure [32]:

$$\Gamma(\theta) = \frac{\hbar^2 k}{\mu}\left(\frac{\phi_{n\ell j}(\bar{r})}{G_\ell(k\bar{r})}\right)^2, \tag{7}$$

where $k = \sqrt{2\mu E}/\hbar$, G_ℓ is the irregular Coulomb wave function, and $\phi_{n\ell j}(r)/r$ is the radial wave function of the bound state, for one orientation angle θ with the inner potential $U(\theta)$. The value of $\bar{r}$ is chosen in such a way that the potential V can be well approximated by the repulsive part (i.e., the attractive part is disregarded) for $r \geqslant \bar{r}$ within a certain θ (see Fig. 1). It should be noted that the decay width $\Gamma(\theta)$ does

not depend on the particular choice of R or $\bar{r}$, as discussed in Refs. [31,32]. Moreover, it is interesting to note that the final expression of the MTPA resembles R-matrix theory, yet without uncertainties related to the choice of the matching radius. There are the further details on the comparison of these two theoretical approaches in Ref. [32].

The radial Schrödinger equation of the bound state with $U(\theta)$, for a certain angle θ, is numerically solved to obtain a corresponding decay width $\Gamma(\theta)$. In this procedure, the depth V_0 is adjusted to reproduce the experimental Q value and the special number of internal nodes determined by the Wildermuth condition [41], which is given by

$$G = 2n + \ell = \sum_{i=1}^{4} g_i. \tag{8}$$

In this expression, n is the number of internal nodes in the radial wave function and g_i are the corresponding oscillator quantum numbers of the nucleons composing the α cluster, whose values are chosen to guarantee that the α cluster outside the shell is occupied entirely by the core nucleus. This is restricted by the Pauli principle. In this case we take the global quantum number $G = 22$ for heavier nuclei with $N > 126$. This is consistent with previous studies [6,13]. For example, we take the α emitter ^{218}Th, a nearly spherical α-daughter system, to present the detailed properties of the bound-state wave function. Here the deformation parameters of the daughter nucleus are taken as $\beta_2 = \beta_4 = 0$, which means this system goes back to a spherical one. As one can see from Fig. 2(a), the wave function has 11 nodes, as expected. Meanwhile, the decimal logarithm of the wave function begins to decrease quickly from a value of about -7 in linear form for $r > R$, as shown in Fig. 2(b). This means that the wave function decreases sharply in magnitude by about 7 orders in the barrier region ($r < R$) and begins to vanish gradually in an exponential law from the separation radius R.

After the angle-dependent decay width $\Gamma(\theta)$ is obtained, the final α-decay width can be obtained by averaging it in all directions:

$$\Gamma = \int_0^{\pi/2} \Gamma(\theta) \sin(\theta)\, d\theta. \tag{9}$$

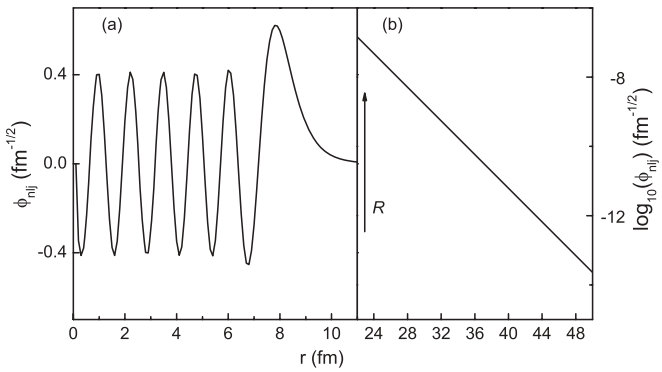

FIG. 2. Schematic plot of the bound-state wave function in the spherical ^{214}Ra + α system in (a) the inner region ($r < R$) and (b) the outer region ($r > R$). The separation radius R is indicated. Note that y axis in (b) is designated the decimal logarithm.

The above procedure for the deformed system has been widely applied in the calculations of both α-decay half-lives and α-capture cross sections [10–12,42,43]. The half-life of α decay can be achieved as

$$T_{1/2} = \frac{\hbar \ln 2}{P_\alpha \Gamma}, \tag{10}$$

where the preformation factor P_α is an indispensable quantity for the calculation. In terms of the nuclear structure, the preformation factor is very important because α decay is a rich source of nuclear structure information. Nevertheless, because of the complexity of both the nuclear potential and the nuclear many-body problem, it is quite difficult to evaluate the value of P_α. The preformation factor α is obtained from the experimental analysis of the (n,α) and (p,α) reactions and α radioactivity of even-even nuclei [25]. It is shown that the preformation factor varies smoothly in the open-shell region and has a value smaller than 1.0. As a result, it is reasonable and appropriate to take the preformation factor as constant for different kinds of nuclei. In the present work its value is taken as follows: $P_\alpha = 0.34$ for even-even nuclei, $P_\alpha = 0.21$ for odd-A nuclei, and $P_\alpha = 0.15$ for odd-odd nuclei. These values agree well with both the microscopic calculation for ^{212}Po and the experimental data of open-shell nuclei [3,25] and the procedure is consistent with the model of Buck *et al.* [4]. There is no doubt that the agreement between the calculated results and the experimental data should be better if the P_α value is taken as a variable with different parent nuclei instead of a constant [34,44]. This is worth further investigation.

III. NUMERICAL RESULTS AND DISCUSSION

For comparison, the well-known Viola-Seaborg formula, which is employed to evaluate α-decay half-lives, is written as [35–37]

$$\log_{10} T_{1/2} = (aZ + b)Q^{-1/2} + (cZ + d) + h, \tag{11}$$

where Z is the proton number of the parent nucleus and h is the hindrance factor for nuclei with unpaired nucleons. Through the best fit to the available experimental data, including the recently synthesized SHEs and isotopes, we obtain the parameters $a = 1.646\,32$, $b = -7.448\,80$, $c = -0.209\,56$, and $d = -33.0187$, which are determined in an adjustment that takes into account the available data for even-even heavy and superheavy nuclei (with $N > 126$ and $Z \geqslant 82$) [21,45–49]. The hindrance factor h is obtained as 0, 0.1367, 0.5172, and 0.5007 for even-even, even-odd, odd-even, and odd-odd nuclei, respectively, through a least-squares fit to the experimental data.

Very recently, Denisov and Khudenko [16] and Royer [17] proposed accurate formulas to evaluate α-decay half-lives. For example, Denisov and Khudenko [16] offer a set of simple relations for the evaluation of the half-lives of α transitions between ground states, which work well for both light and heavy α emitters. Considering the recent progress in the experimental synthesis of SHEs and isotopes [21,47], it is of interest to use their relations to calculate the α-decay half-lives of heavy and superheavy nuclei. Based on the formula in

Ref. [16], a different fitting of the parameters is made where the recent data of superheavy nuclei are also included. For 77 even-even, 40 even-odd, 42 odd-even, and 29 odd-odd nuclei, we find that available experimental α-decay half-lives can be well reproduced with the following parameters for the formulas [16]:

$$\log_{10}\left(T_{1/2}^{e\text{-}e}\right)=-26.7517-1.1046(A-4)^{1/6}Z^{1/2}+\frac{1.5826Z}{\sqrt{Q}}, \tag{12}$$

$$\log_{10}\left(T_{1/2}^{e\text{-}o}\right) = -26.7321-1.2597(A-4)^{1/6}Z^{1/2}+\frac{1.7071Z}{\sqrt{Q}} + \frac{0.7775\sqrt{\ell(\ell+1)}}{QA^{-1/6}} - 0.7689[(-1)^{\ell}-1], \tag{13}$$

$$\log_{10}\left(T_{1/2}^{o\text{-}e}\right) = -29.5599-1.1342(A-4)^{1/6}Z^{1/2}+\frac{1.7040Z}{\sqrt{Q}} + \frac{0.3693\sqrt{\ell(\ell+1)}}{QA^{-1/6}} - 0.5760[(-1)^{\ell}-1], \tag{14}$$

$$\log_{10}\left(T_{1/2}^{o\text{-}o}\right) = -23.9210-1.1798(A-4)^{1/6}Z^{1/2}+\frac{1.5720Z}{\sqrt{Q}} + \frac{0.9678\sqrt{\ell(\ell+1)}}{QA^{-1/6}} - 0.1937[(-1)^{\ell}-1]. \tag{15}$$

The present study is initially restricted to the ground-state (g.s.) to g.s. α transitions of even-even heavy nuclei with $N > 126$. Consequently, it is reasonable to take these transitions as favored α decays. The experimental data and the calculated α-decay half-lives for even-even heavy nuclei with $A < 260$ are listed in Table I. These experimental values, such as decay energies and half-lives, are mainly taken from Refs. [45,46]. In Table I the first and second columns list the elemental symbol and the mass number of the parent nucleus, respectively. The third and fourth columns are, respectively, the experimental decay energies and partial half-lives for the g.s. to g.s. α transitions. The numerical results obtained with the MTPA, the Viola-Seaborg formula, and the empirical relations of Ref. [16] are presented in the last three columns, respectively. Note that the results of the empirical formulas are calculated with the parameter values from the present work. As seen from Table I, the calculated half-lives are found to be in good agreement with the experimental data, although the α-decay half-lives span a large order of magnitude.

For further insight, we give a comparison of the calculated results with the experimental data for different isotopic chains in Fig. 3. One can see that the absolute values of $\log_{10}(T_{1/2}^{\rm calc}/T_{1/2}^{\rm expt})$ are generally less than 0.4, which corresponds to the values of $T_{1/2}^{\rm calc}/T_{1/2}^{\rm expt}$ in the range of about 0.4–2.5. The slightly large deviation is for the parent nucleus ^{210}Pb, which may be caused by the effect of the $Z = 82$ closed shell. This effect results in a decrease of the α-preformation factor, which has been shown in the experimental analysis [25].

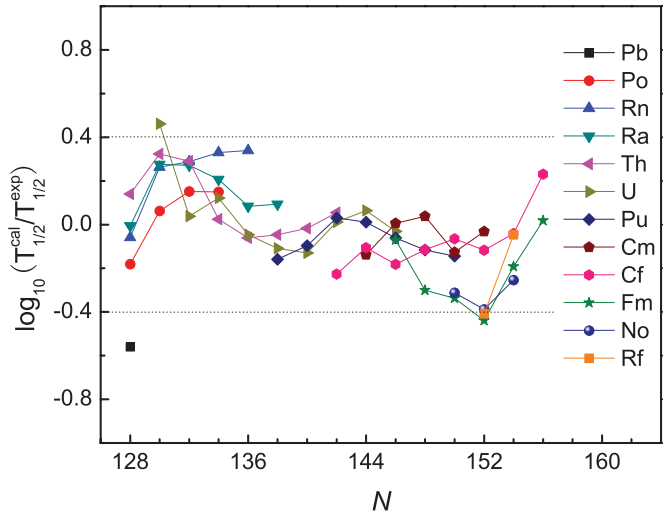

FIG. 3. (Color online) Decimal logarithm of $T_{1/2}^{\rm calc}/T_{1/2}^{\rm expt}$ versus the neutron number N for even-even heavy nuclei with $N > 126$. The values 0.2 and 0.4 of the decimal logarithms correspond to the absolute deviations of the half-lives with factors of 1.6 and 2.5, respectively.

It is obvious that a fixed value of the preformation factor cannot describe the features of the nuclear structure. Nevertheless, the systematic trend of the agreement between the calculated and measured α-decay half-lives for different isotopic and isotonic chains can provide some information on the properties of the nuclear structure. As shown in Fig. 3, the deviation of $\log_{10}(T_{1/2}^{\rm calc}/T_{1/2}^{\rm expt})$ increases from the neutron number $N = 128$ for several isotopic chains, which results from the influence of the spherical shell closure $N = 126$. Meanwhile, the effect of the deformed shell $N = 152$ is clear [15,30]. The deviations of the agreement between calculations and experiments at $N = 152$ are obviously smaller than those of the neighboring region. Similarly, we also plot the deviations of $N = 128$–156 isotones versus the proton number of the parent nucleus. In Fig. 4 one can see that the deviations for different isotones generally increase with the proton number moving away from the spherical shell closure $Z = 82$ and in general decrease with the proton number approaching the deformed $Z = 100$ shell [30].

For the 64 even-even heavy nuclei, the value of the standard deviation is 0.21, which is defined as $\sqrt{\langle\sigma^2\rangle} = \sqrt{\frac{1}{N}\sum_{i=1}^{N}(\log_{10}T_{\rm calc}^{i}-\log_{10}T_{\rm expt}^{i})^2}$. This means that there is good agreement between the calculated α-decay half-lives and the experimental data within a mean factor of 2. In light of this, we also extend this study to the superheavy region including the SHEs. This can be considered as a further test of the validity and applicability of the present method. Considering that there is little knowledge of the level schemes in the superheavy mass region, the angular momentum of the emitted α particle for superheavy nuclei is assumed to be $\ell = 0$ (i.e., a favored α transition).

Table II displays the detailed numerical results of the observed α-decay chains originating from the recently synthesized SHEs. The experimental data are mostly taken from

TABLE I. Comparison of the experimental and calculated α-decay half-lives for even-even heavy nuclei with neutron number $N > 126$. The last two columns are the results obtained with the Viola-Seaborg formula (denoted by form 1) and the empirical relations of Denisov and Khudenko (denoted by form 2), respectively, for which calculations are performed with the present set of parameters.

Element	A	Q(MeV)	$T_{1/2}^{\text{expt}}$(s)	$T_{1/2}^{\text{calc}}$(s)	$T_{1/2}^{\text{form 1}}$(s)	$T_{1/2}^{\text{form 2}}$(s)
Pb	210	3.792	3.69×10^{16}	1.02×10^{16}	1.98×10^{15}	3.82×10^{15}
Po	212	8.954	2.99×10^{-7}	1.74×10^{-7}	1.27×10^{-7}	1.08×10^{-7}
	214	7.833	1.64×10^{-4}	1.67×10^{-4}	1.34×10^{-4}	1.16×10^{-4}
	216	6.906	1.45×10^{-1}	1.81×10^{-1}	1.47×10^{-1}	1.30×10^{-1}
	218	6.115	1.86×10^{2}	2.31×10^{2}	1.95×10^{2}	1.77×10^{2}
Rn	214	9.208	2.70×10^{-7}	2.08×10^{-7}	1.45×10^{-7}	1.34×10^{-7}
	216	8.200	4.50×10^{-5}	7.28×10^{-5}	6.32×10^{-5}	5.81×10^{-5}
	218	7.263	3.50×10^{-2}	5.99×10^{-2}	5.38×10^{-2}	4.99×10^{-2}
	220	6.405	5.56×10^{1}	1.05×10^{2}	9.11×10^{1}	8.62×10^{1}
	222	5.590	3.31×10^{5}	6.38×10^{5}	4.92×10^{5}	4.83×10^{5}
Ra	216	9.526	1.82×10^{-7}	1.59×10^{-7}	1.16×10^{-7}	1.17×10^{-7}
	218	8.546	2.56×10^{-5}	4.26×10^{-5}	3.55×10^{-5}	3.52×10^{-5}
	220	7.592	1.81×10^{-2}	2.98×10^{-2}	2.61×10^{-2}	2.58×10^{-2}
	222	6.679	3.92×10^{1}	5.57×10^{1}	5.20×10^{1}	5.21×10^{1}
	224	5.789	3.33×10^{5}	4.04×10^{5}	4.54×10^{5}	4.70×10^{5}
	226	4.871	5.35×10^{10}	6.63×10^{10}	6.42×10^{10}	7.13×10^{10}
Th	218	9.849	1.17×10^{-7}	1.33×10^{-7}	9.12×10^{-8}	1.01×10^{-7}
	220	8.953	9.70×10^{-6}	1.80×10^{-5}	1.41×10^{-5}	1.52×10^{-5}
	222	8.127	2.29×10^{-3}	3.53×10^{-3}	3.04×10^{-3}	3.19×10^{-3}
	224	7.298	1.33×10^{0}	1.41×10^{0}	1.62×10^{0}	1.68×10^{0}
	226	6.451	2.43×10^{3}	2.14×10^{3}	3.35×10^{3}	3.48×10^{3}
	228	5.520	8.35×10^{7}	7.63×10^{7}	1.04×10^{8}	1.12×10^{8}
	230	4.770	3.12×10^{12}	3.00×10^{12}	3.56×10^{12}	4.00×10^{12}
	232	4.082	5.67×10^{17}	6.45×10^{17}	5.89×10^{17}	7.01×10^{17}
U	222	9.500	1.25×10^{-6}	3.68×10^{-6}	2.66×10^{-6}	3.13×10^{-6}
	224	8.620	7.29×10^{-4}	7.96×10^{-4}	5.65×10^{-4}	6.43×10^{-4}
	226	7.701	4.12×10^{-1}	3.56×10^{-1}	3.95×10^{-1}	4.41×10^{-1}
	228	6.803	8.45×10^{2}	5.17×10^{2}	8.23×10^{2}	9.14×10^{2}
	230	5.993	2.67×10^{6}	2.08×10^{6}	3.38×10^{6}	3.76×10^{6}
	232	5.414	3.19×10^{9}	2.37×10^{9}	3.93×10^{9}	4.33×10^{9}
	234	4.858	1.08×10^{13}	1.12×10^{13}	1.10×10^{13}	1.21×10^{13}
	236	4.573	1.00×10^{15}	1.16×10^{15}	1.11×10^{15}	1.18×10^{15}
	238	4.270	1.78×10^{17}	1.66×10^{17}	2.48×10^{17}	2.56×10^{17}
Pu	232	6.716	1.33×10^{4}	1.19×10^{4}	1.33×10^{4}	1.52×10^{4}
	234	6.310	7.73×10^{5}	6.19×10^{5}	8.39×10^{5}	9.16×10^{5}
	236	5.867	1.30×10^{8}	1.40×10^{8}	1.25×10^{8}	1.31×10^{8}
	238	5.593	3.90×10^{9}	4.00×10^{9}	3.71×10^{9}	3.69×10^{9}
	240	5.256	2.84×10^{11}	2.47×10^{11}	3.43×10^{11}	3.27×10^{11}
	242	4.985	1.54×10^{13}	1.16×10^{13}	1.81×10^{13}	1.65×10^{13}
	244	4.666	3.17×10^{15}	2.27×10^{15}	2.99×10^{15}	2.63×10^{15}
Cm	240	6.398	3.29×10^{6}	2.40×10^{6}	2.52×10^{6}	2.56×10^{6}
	242	6.216	1.90×10^{7}	1.92×10^{7}	1.85×10^{7}	1.75×10^{7}
	244	5.902	7.43×10^{8}	8.17×10^{8}	7.13×10^{8}	6.40×10^{8}
	246	5.475	1.83×10^{11}	1.36×10^{11}	1.68×10^{11}	1.45×10^{11}
	248	5.162	1.46×10^{13}	1.33×10^{13}	1.40×10^{13}	1.16×10^{13}
Cf	240	7.719	9.74×10^{1}	5.39×10^{1}	6.82×10^{1}	7.74×10^{1}
	242	7.517	2.62×10^{2}	2.05×10^{2}	3.74×10^{2}	3.94×10^{2}
	244	7.329	2.22×10^{3}	1.46×10^{3}	1.94×10^{3}	1.90×10^{3}
	246	6.862	1.62×10^{5}	1.24×10^{5}	1.55×10^{5}	1.44×10^{5}
	248	6.361	3.60×10^{7}	3.05×10^{7}	2.89×10^{7}	2.56×10^{7}
	250	6.128	4.87×10^{8}	3.73×10^{8}	4.07×10^{8}	3.38×10^{8}
	252	6.217	1.02×10^{8}	9.28×10^{7}	1.46×10^{8}	1.10×10^{8}
	254	5.927	2.03×10^{9}	3.47×10^{9}	4.52×10^{9}	3.23×10^{9}

TABLE I. (*Continued*)

Element	A	Q(MeV)	$T_{1/2}^{\text{expt}}$(s)	$T_{1/2}^{\text{calc}}$(s)	$T_{1/2}^{\text{form 1}}$(s)	$T_{1/2}^{\text{form 2}}$(s)
Fm	246	8.374	1.49×10^{0}	1.27×10^{0}	2.20×10^{0}	2.31×10^{0}
	248	8.002	4.84×10^{1}	2.28×10^{1}	3.90×10^{1}	3.82×10^{1}
	250	7.557	2.65×10^{3}	1.05×10^{3}	1.60×10^{3}	1.47×10^{3}
	252	7.153	1.09×10^{5}	3.97×10^{4}	6.25×10^{4}	5.43×10^{4}
	254	7.308	1.37×10^{4}	8.80×10^{3}	1.48×10^{4}	1.17×10^{4}
	256	7.027	1.35×10^{5}	1.41×10^{5}	2.09×10^{5}	1.54×10^{5}
No	252	8.550	4.71×10^{0}	2.00×10^{0}	3.07×10^{0}	3.10×10^{0}
	254	8.226	7.08×10^{1}	2.89×10^{1}	3.61×10^{1}	3.40×10^{1}
	256	8.581	3.36×10^{0}	1.87×10^{0}	2.44×10^{0}	2.08×10^{0}
Rf	256	8.930	2.38×10^{0}	7.87×10^{-1}	9.76×10^{-1}	1.04×10^{0}
	258	9.250	9.23×10^{-2}	8.27×10^{-2}	1.08×10^{-1}	1.04×10^{-1}

Refs. [21,47–49], including the element $Z = 117$ [21], several isotopes [48], and data with improved accuracy [49]. The SHE experiments are very difficult and usually few decay events are observed. Hence the experimental error bar is relatively large in the measurement of both decay energies and half-lives. Despite this, the experimental α-decay half-lives are well reproduced

TABLE II. Same as Table I but for the recently observed α-decay chains of the SHEs. [a]Half-lives deduced from the only event of the observed $^{294}117$ decay chain. [b]Uncertain experimental error bar.

Element	A	Q(MeV)	$T_{1/2}^{\text{expt}}$	$T_{1/2}^{\text{calc}}$	$T_{1/2}^{\text{form 1}}$	$T_{1/2}^{\text{form 2}}$
118	294	11.81(6)	$0.89^{+1.07}_{-0.31}$ ms	1.05 ms	0.41 ms	0.52 ms
116	290	11.00(8)	$7.1^{+3.2}_{-1.7}$ ms	10.9 ms	10.2 ms	11.6 ms
114	286	10.33(6)	$0.26^{+0.08}_{-0.04}$ s	0.17 s	0.15 s	0.15 s
117	293	11.18(8)	14^{+11}_{-4} ms	15 ms	23 ms	33 ms
115	289	10.46(9)	$0.22^{+0.26}_{-0.08}$ s	0.23 s	0.43 s	0.67 s
113	285	9.88(8)	$5.5^{+5.0}_{-1.8}$ s	2.0 s	4.3 s	7.0 s
117	294	10.96(10)	78^{+370}_{-36} ms	66 ms	79 ms	63 ms
115	290	10.09(40)	0.023 s[a]	2.5 s	4.4 s	3.3 s
113	286	9.77(10)	28.3 s	5.5 s	8.6 s	6.2 s
111	282	9.13(10)	0.74 s[a]	86.80 s	171.33 s	117.44 s
109	278	9.69(10)	11.0 s[a]	0.6 s	0.8 s	0.5 s
107	274	8.93(10)	1.3 min[a]	0.3 min	0.5 min	0.4 min
116	293	10.69(6)	61^{+57}_{-20} ms	121 ms	87 ms	89 ms
114	289	10.01(3)	$2.1^{+0.8}_{-0.4}$ s	1.7 s	2.2 s	1.9 s
112	285	9.34(3)	29^{+11}_{-6} s	33 s	54 s	51 s
110	281	8.86(3)	144^{+250}_{-12} s	190 s	253 s	420 s
116	292	10.80(7)	18^{+16}_{-6} ms	34 ms	33 ms	35 ms
114	288	10.08(6)	$0.80^{+0.27}_{-0.16}$ s	1.02 s	0.72 s	0.69 s
112	284	9.349(50)	$9.8^{+18}_{-3.8}$ s	17.4 s	23.9 s	20.8 s
115	288	10.61(6)	87^{+105}_{-30} ms	174 ms	166 ms	138 ms
113	284	10.15(6)	$0.48^{+0.58}_{-0.17}$ s	0.60 s	0.72 s	0.57 s
111	280	9.87(6)	$3.6^{+4.3}_{-1.3}$ s	0.53 s	1.04 s	0.80 s
115	287	10.74(9)	32^{+155}_{-14} ms	59 ms	79 ms	118 ms
113	283	10.26(9)	100^{+490}_{-45} ms	155 ms	373 ms	543 ms
111	279	10.52(16)	170^{+810}_{-80} ms	11 ms	19 ms	19 ms
113	282	10.78(8)	73^{+134}_{-29} ms	10 ms	16 ms	14 ms
111	278	10.85(8)	$4.2^{+7.5}_{-1.7}$ ms	2.2 ms	2.7 ms	2.4 ms
110	270	11.20(5)	100^{+140}_{-40} μs	54 μs	65 μs	77 μs
108	266	10.336(20)	$2.3^{+1.3}_{-0.6}$ ms	1.9 ms	2.2 ms	2.4 ms
108	270	9.02(3)	$3.6^{+0.8}_{-1.4}$ s	6.9 s	11.7 s	11.2 s
106	266	8.76(5)	25.7 s[b]	8.9 s	16.3 s	14.5 s
108	264	10.591(20)	0.85 ms[b]	0.43 ms	0.49 ms	0.59 ms
106	260	9.92(3)	$9.5^{+2.1}_{-1.4}$ ms	4.4 ms	6.4 ms	7.1 ms

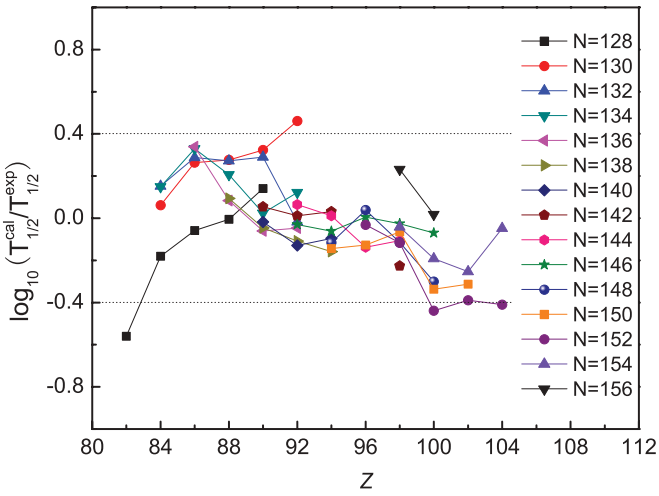

FIG. 4. (Color online) Deviations between the calculated and measured half-lives versus the proton number Z for the even-even isotones, which show the effects of the spherical shell $Z = 82$ and the deformed shell $Z = 100$.

in the present study, except for the $^{294}117$ decay chain. In particular, the discrepancy between theory and experiment is obviously large for $^{282}111$ and $^{290}115$. As mentioned in Ref. [21], only one decay event is observed originating from the isotope $^{294}117$ in the synthesized experiment. In addition, the experimental error bar of the Q value for $^{290}115$ is 0.40 MeV, which could cause large uncertainty in the calculation of α-decay half-lives. It will be interesting to investigate the cause of this discrepancy in detail. In general, as shown in the tables, the MTPA within a deformed version of the cluster model gives a good description of α decay.

IV. CONCLUSION

In summary, the modified two-potential approach is employed and extended to give a systematic calculation of the α-decay half-lives of even-even heavy nuclei within the cluster model, taking into account the nuclear deformation effect. The deformation-dependent α-nucleus potential is applied to evaluate the α-decay width. We also extend the calculation to the observed α-decay chains of recently synthesized SHEs and isotopes. The α preformation factor is considered constant for each kind of nucleus. The shell effect on α transitions is also discussed to some extent. Moreover, we have evaluated the α-decay half-lives in the empirical formulas for comparison. As shown in Tables I and II, there is good agreement between the calculated half-lives and the experimental data. The present work has the potential to be extended to further investigation of α-decay properties within reasonable nuclear structure models.

ACKNOWLEDGMENTS

This work was supported by the National Natural Science Foundation of China (Grants No. 11035001, No. 10735010, and No. 10975072), the 973 National Major State Basic Research and Development of China (Grants No. 2007CB815004 and No. 2010CB327803), CAS Knowledge Innovation Project No. KJCX2-SW-N02, and Research Fund of Doctoral Point, Grant No. 20100091110028.

[1] G. Gamow, Z. Phys. **51**, 204 (1928).
[2] E. U. Condon and R. W. Gurney, Nature (London) **122**, 439 (1928).
[3] K. Varga, R. G. Lovas, and R. J. Liotta, Phys. Rev. Lett. **69**, 37 (1992).
[4] B. Buck, A. C. Merchant, and S. M. Perez, At. Data Nucl. Data Tables **54**, 53 (1993).
[5] P. Mohr, Phys. Rev. C **73**, 031301(R) (2006).
[6] J. C. Pei, F. R. Xu, Z. J. Lin, and E. G. Zhao, Phys. Rev. C **76**, 044326 (2007).
[7] G. Royer, J. Phys. G: Nucl. Part. Phys. **26**, 1149 (2000).
[8] N. G. Kelkar and H. M. Castañeda, Phys. Rev. C **76**, 064605 (2007).
[9] P. R. Chowdhury, C. Samanta, and D. N. Basu, Phys. Rev. C **77**, 044603 (2008).
[10] C. Xu and Z. Ren, Phys. Rev. C **73**, 041301(R) (2006); **74**, 014304 (2006).
[11] V. Yu. Denisov and A. A. Khudenko, At. Data Nucl. Data Tables **95**, 815 (2009).
[12] K. P. Santhosh, Sabina Sahadevan, and Jayesh George Joseph, Nucl. Phys. A **850**, 34 (2011).
[13] D. Ni and Z. Ren, Nucl. Phys. A **825**, 145 (2009).
[14] D. S. Delion, S. Peltonen, and J. Suhonen, Phys. Rev. C **73**, 014315 (2006).
[15] D. Ni and Z. Ren, Phys. Rev. C **81**, 024315 (2010); **81**, 064318 (2010).
[16] V. Yu. Denisov and A. A. Khudenko, Phys. Rev. C **79**, 054614 (2009); **82**, 059901(E) (2010).
[17] G. Royer, Nucl. Phys. A **848**, 279 (2010).
[18] S. Hofmann and G. Münzenberg, Rev. Mod. Phys. **72**, 733 (2000).
[19] T. N. Ginter *et al.*, Phys. Rev. C **67**, 064609 (2003).
[20] Yu. Ts. Oganessian *et al.*, Phys. Rev. C **72**, 034611 (2005); **74**, 044602 (2006).
[21] Yu. Ts. Oganessian *et al.*, Phys. Rev. Lett. **104**, 142502 (2010).
[22] M. Freer *et al.*, Phys. Rev. Lett. **96**, 042501 (2006).
[23] K. Toth *et al.*, Phys. Rev. Lett. **53**, 1623 (1984).
[24] J. Wauters *et al.*, Phys. Rev. Lett. **72**, 1329 (1994).
[25] P. E. Hodgson and E. Běták, Phys. Rep. **374**, 1 (2003).
[26] R. G. Lovas, R. J. Liotta, A. Insolia, K. Varga, and D. S. Delion, Phys. Rep. **294**, 265 (1998).
[27] A. N. Andreyev *et al.*, Nature (London) **405**, 430 (2000).
[28] D. S. Delion, A. Sandulescu, and W. Greiner, Phys. Rev. C **69**, 044318 (2004).
[29] H. F. Zhang and G. Royer, Phys. Rev. C **77**, 054318 (2008).
[30] G. L. Zhang, X. Y. Le, and H. Q. Zhang, Nucl. Phys. A **823**, 16 (2009).
[31] S. A. Gurvitz and G. Kalbermann, Phys. Rev. Lett. **59**, 262 (1987).
[32] S. A. Gurvitz, P. B. Semmes, W. Nazarewicz, and T. Vertse, Phys. Rev. A **69**, 042705 (2004).

[33] Y. Qian, Z. Ren, and D. Ni, J. Phys. G: Nucl. Part. Phys. **38**, 015102 (2011).
[34] Y. Qian and Z. Ren, Nucl. Phys. A **852**, 82 (2011).
[35] V. E. Viola Jr. and G. T. Seaborg, J. Inorg. Nucl. Chem. **28**, 741 (1966).
[36] P. Möller, J. R. Nix, and K. L. Kratz, At. Data Nucl. Data Tables **66**, 131 (1997).
[37] T. Dong and Z. Ren, Eur. Phys. J. A **26**, 69 (2005).
[38] Z. Ren, C. Xu, and Z. Wang, Phys. Rev. C **70**, 034304 (2004).
[39] P. Mohr, Open Nucl. Part. Phys. J. **1**, 1 (2008).
[40] P. Möller, J. R. Nix, W. D. Myers, and W. J. Swiatecki, At. Data Nucl. Data Tables **59**, 185 (1995).
[41] K. Wildermuth and Y. C. Tang, *A Unified Theory of the Nucleus* (Academic, New York, 1997).
[42] T. L. Stewart, M. W. Kermode, D. J. Beachey, N. Rowley, I. S. Grant, and A. T. Kruppa, Nucl. Phys. A **611**, 332 (1996).
[43] V. Yu. Denisov and H. Ikezoe, Phys. Rev. C **72**, 064613 (2005).
[44] Z. Ren and G. Xu, J. Phys. G: Nucl. Part. Phys. **15**, 465 (1989).
[45] G. Audi, O. Bersillon, J. Blachot, and A. H. Wapstra, Nucl. Phys. A **729**, 3 (2003).
[46] National Nuclear Data Center, Brookhaven National Laboratory [http://www.nndc.bnl.gov].
[47] Yu. Ts. Oganessian and S. N. Dmitriev, Russ. Chem. Rev. **78**, 1077 (2009).
[48] K. Nishio *et al.*, Phys. Rev. C **82**, 024611 (2010).
[49] Ch. E. Düllmann *et al.*, Phys. Rev. Lett. **104**, 252701 (2010).